



Very high-rate GPS for measuring dynamic seismic displacements without aliasing: performance evaluation of the variometric approach

Yuanming Shu¹ · Rongxin Fang¹ · Min Li¹ · Chuang Shi^{1,2} · Meng Li³ · Jingnan Liu¹

Received: 9 January 2018 / Accepted: 11 September 2018 / Published online: 18 September 2018
© Springer-Verlag GmbH Germany, part of Springer Nature 2018

Abstract

Very high-rate global positioning system (GPS) data has the capacity to quickly resolve seismically related ground displacements, thereby providing great potential for rapidly determining the magnitude and the nature of an earthquake's rupture process and for providing timely warnings for earthquakes and tsunamis. The GPS variometric approach can measure ground displacements with comparable precision to relative positioning and precise point positioning (PPP) within a short period of time. The variometric approach is based on single-differencing over time of carrier phase observations using only the broadcast ephemeris and a single receiver to estimate velocities, which are then integrated to derive displacements. We evaluate the performance of the variometric approach to measure displacements using 50 Hz GPS data, which were recorded during the 2013 M_w 6.6 Lushan earthquake and the 2011 M_w 9.0 Tohoku-Oki earthquake. The comparison between 50 and 1 Hz seismic displacements demonstrates that 1 Hz solutions often fail to faithfully manifest the seismic waves containing high-frequency seismic signals due to aliasing, which is common for near-field stations of a moderate-magnitude earthquake. Results indicate that 10–50 Hz sampling GPS sites deployed close to the source or the ruptured fault are needed for measuring dynamic seismic displacements of moderate-magnitude events. Comparisons with post-processed PPP results reveal that the variometric approach can determine seismic displacements with accuracies of 0.3–4.1, 0.5–2.3 and 0.8–6.8 cm in the east, north and up components, respectively. Moreover, the power spectral density analysis demonstrates that high-frequency noises of seismic displacements, derived using the variometric approach, are smaller than those of PPP-derived displacements in these three components.

Keywords Very high-rate GPS · Seismic displacements · Variometric approach · Aliasing

Introduction

High-rate global positioning system (GPS) has long been used to directly measure dynamic ground displacements generated by earthquakes complementary to seismic records,

which has a great potential to contribute to rapid magnitude determination (Wright et al. 2012; Fang et al. 2014; Melgar et al. 2015), rupture process inversion (Miyazaki et al. 2004; Grapenthin and Freymueller 2011), as well as earthquake and tsunami early warning systems (Crowell et al. 2009; Allen and Ziv 2011; Colombelli et al. 2013). Since the first demonstration of the capability of high-rate GPS to recover seismic waves induced by strong earthquakes (Larson et al. 2003), interests in GPS seismology have been continuously growing (Bilich et al. 2008; Larson 2009; Yin and Wdowinski 2013). With GPS kinematic positioning techniques, arbitrarily large dynamic displacements can be obtained at near-source GPS stations without the saturation problem experienced by traditional seismic sensors (Bock et al. 2004).

There are three main GPS kinematic positioning approaches to estimate seismic displacements: relative positioning, precise point positioning (PPP, Zumberge et al.

Electronic supplementary material The online version of this article (<https://doi.org/10.1007/s10291-018-0785-z>) contains supplementary material, which is available to authorized users.

✉ Rongxin Fang
rxfang@whu.edu.cn

¹ GNSS Research Center, Wuhan University, Wuhan 430079, China

² School of Electronic and Information Engineering, Beihang University, 37 Xueyuan Road, Beijing 100083, China

³ Faculty of Geomatic, East China Institute of Technology, Nanchang 330013, China

1997) and the variometric approach (Colosimo et al. 2011). In relative positioning, double-differenced carrier phase observations between stations, usually including at least one reference station, are used to achieve centimeter or even millimeter level accuracy of GPS precise positioning (Bock et al. 2011; Ohta et al. 2012). The benefit of this approach is that most of the GPS positioning errors are canceled by double-differenced measurement equations for a relatively short baseline. The weakness of this approach is that absolute seismic displacements will not be estimated accurately if the reference stations also experience seismic motions. It is also not appropriate to choose reference stations far from the earthquake monitoring area since the positioning accuracy in the relative positioning degrades as the baseline length increases.

PPP can provide kinematic positioning results at centimeter level accuracy without the requirement for specific reference stations and has been widely used to retrieve seismic displacements (Kouba 2003; Xu et al. 2013). However, PPP relies on precise satellite orbit and clock products. The freely available GPS precise orbit and clock products generated by IGS (International GNSS Service) have undesirable latencies ranging from 17 to 41 h for rapid products to 12–18 days for final products, while ultra-rapid and real-time orbit/clock products may suffer from degraded precision or communication failure of the real-time data stream. Besides, a relatively long convergence or re-convergence time of around 20–30 min are needed for PPP to achieve centimeter-level positioning accuracy (Heroux and Kouba 2001), which is intolerable for real-time GPS applications such as GPS-based earthquake early warning and GPS meteorology.

The variometric approach estimates velocities and displacements using a single receiver and standard GPS broadcast ephemeris which are routinely available in real time. Extensive experiments have been conducted demonstrating that this approach can determine velocities and displacements with accuracies of a few millimeters per second and a few centimeters, respectively (Colosimo et al. 2011; Branzanti et al. 2013; Benedetti et al. 2014; Li et al. 2014; Geng et al. 2016). This approach has advantages over relative positioning and PPP because neither any reference station(s) nor precise orbit and clock products are needed. Besides, there is no need to estimate carrier phase ambiguities because they are canceled through time differences, thus the convergence process is eliminated. Moreover, compared to PPP, the variometric approach has the advantage to be used with L1 observations only, with a very little degradation of the final results (Benedetti et al. 2014).

Over the past decade, GPS data with sampling rates of 1 Hz were regularly obtained to detect earthquake-related displacements. According to the Nyquist theorem, if real signals have energy at frequencies above half the sampling frequency which is denoted as the Nyquist frequency, then

the sampled data will be aliased (Nyquist 1928; Smalley 2009). In the aliasing effect, the signals above the Nyquist frequency are correctly recorded instantaneously, but they will masquerade as lower frequencies in the time and frequency domains of the sampled data. Therefore, 1 Hz GPS data is only sufficient to recover signals at frequencies below 0.5 Hz. Nevertheless, the dominant frequency could exceed 0.5 Hz in some situations such as the dynamics of tall buildings, towers, and large suspension bridges during earthquakes, high winds and traffic loading (Celebi and Sanli 2002; Ogaja et al. 2007; Avallone et al. 2011; Moschas and Stiros 2015). Larson (2009) indicated that 1 Hz sampling is simply not sufficient if GPS is going to be a valuable tool for measuring dynamic seismic displacements due to the problem of aliasing. Smalley (2009) demonstrated that 1 Hz GPS recordings of dynamic displacements at very small epicentral distances within several kilometers from an earthquake with the magnitude as small as M_w 6 are aliased, and sampling at 5 Hz might also be aliased for M_w 7 and larger earthquakes. He also pointed out that these aliasing problems are limited only to the stations that are extremely close to the fault. Many researchers in both the seismology and engineering fields have expressed the desire for GPS data with a 10 Hz or higher sampling rate to acquire high-frequency displacement information.

Although some researches have been conducted to assess the performance of very high-rate GPS and the improvement in resolution for GPS displacements, the analysis approaches are mostly relative positioning and PPP (Genrich and Bock 2006; Xu et al. 2013; Avallone et al. 2011). Up to present, there are few reports on the very high-rate GPS analysis based on the variometric approach, with the study of Hung et al. (2017) being the first. By analyzing 1–50 Hz GPS data during the 2013 M_L 6.4 Ruisui earthquake using the variometric approach as well as relative positioning and PPP, they verified the capability of very high-rate GPS in retrieving reliable seismic waveforms through the comparison with seismic instruments. Further studies are needed on the performance of the variometric approach in its applications to very high-rate GPS data.

In this study, we will evaluate the performance of the variometric approach to measure dynamic displacements using very high-rate GPS data. The 50 Hz GPS recordings during two real-world events, i.e., the 2013 M_w 6.6 Lushan earthquake and the 2011 M_w 9.0 Tohoku-Oki earthquake, will be used to investigate the problems of aliasing of 1 Hz GPS seismograms.

We first briefly describe the variometric approach, followed by the description of the 50 Hz GPS data used in this study. Then we present the comparison between 50 and 1 Hz displacements derived using the variometric approach, as well as the comparison between the variometric approach and PPP. Conclusions are given in the last section.

The variometric approach

The variometric approach can estimate seismic waveforms in real time with a stand-alone GPS receiver. Based on single-differencing over time of GPS carrier phase observations, the variometric approach first estimates the change of receiver coordinates between two adjacent epochs, denoted as the “incremental displacements” in the following, and then integrates them to displacements. Note that the velocities can be obtained by dividing the incremental displacements by the time interval. For more details please refer to Colosimo et al. (2011), Branzanti et al. (2013), Benedetti et al. (2014) and Li et al. (2014).

When reconstructing the displacements by a discrete integration of incremental displacements, uncompensated errors may accumulate over time and display their signature as a trend in the displacements. The trend can severely degrade the accuracies of the displacements, thus it is quite crucial to detrend the displacements. Colosimo et al. (2011) presented the strategy of linear trend removal, with which the displacements can achieve centimeter-level accuracy. Recognizing that the trend is caused by common-mode effects on close GPS stations mainly driven by satellite orbit and clock errors, Hung et al. (2017) applied the spatial filtering to mitigate both the linear and non-linear trends in the displacements and achieved the accuracies of very few centimeters. More recently, Fratarcangeli et al. (2018) proposed additional refinement to the variometric approach to eliminate the effect of orbital and clock errors and demonstrated the possibility to estimate coseismic displacements in real time.

We have implemented the software of the variometric approach, following the detrending strategy of Colosimo et al. (2011) to remove the linear trend in the displacements. This implemented software is used to process the GPS data in this study.

Data collection

To fully analyze the performance of the variometric approach to measure displacements using very high-rate GPS data, we considered two events in our study, a moderate one and a large one. The moderate event is the Lushan earthquake that occurred in China at 00:02:47 (UTC) on April 20, 2013 with a magnitude of M_W 6.6 and a depth of 14 km. The large event is the Tohoku-Oki earthquake that occurred in Japan at 05:46:24 (UTC) on March 11, 2011 with a magnitude of M_W 9.0.

Ten 50 Hz GPS stations recording the 2013 M_W 6.6 Lushan earthquake, and five 50 Hz GPS stations recording the 2011 M_W 9.0 Tohoku-Oki earthquake were analyzed

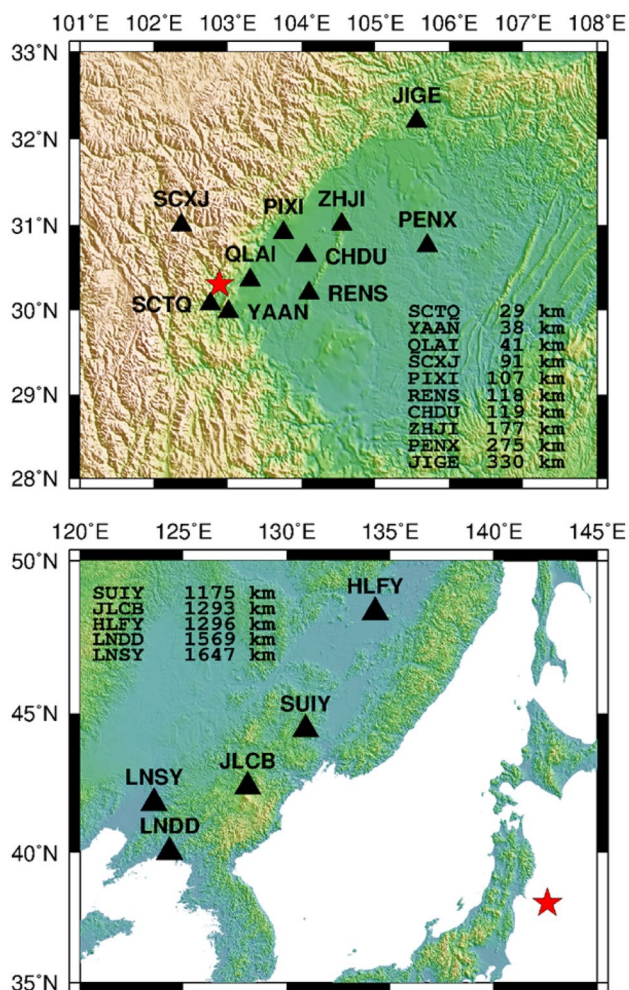


Fig. 1 Distribution of 50 Hz GPS stations recording two earthquakes considered in this study. The black triangles denote the GPS stations, and the red stars represent the epicenters. The epicentral distances of these stations are also shown on the maps. The top and bottom panels represent the GPS stations recording the 2013 M_W 6.6 Lushan earthquake and the 2011 M_W 9.0 Tohoku-Oki earthquake, respectively

in our study. The distribution of these stations and their epicentral distances are shown in Fig. 1. The 10 stations recording the Lushan earthquake are located in China’s Sichuan Province with epicentral distances between 29 and 330 km. The 5 stations recording the Tohoku-Oki earthquake are located in northeast China with epicentral distances ranging from 1175 to 1647 km.

Results and discussion

In this section, we will first assess the variometric approach to capture seismic signals by comparing 50 Hz and 1 Hz results in time and frequency domains. After that, the variometric approach is compared with one of the well-established

GPS positioning techniques, i.e., PPP. When processing the GPS data with the variometric approach, only L1 single-frequency carrier phase observations were used, since the accuracy level of L1 single-frequency solutions is comparable with that of dual-frequency solutions.

Detrending the displacements

To illustrate the effectiveness of the linear-trend removal strategy, we processed 5-min length of GPS data at the station SCTQ during a static period previous to the Lushan earthquake, using the variometric approach without and with detrending. Figure 2 shows the displacements without and with linear trend removal. The original displacements without detrending undergo severe drifts, reaching a few decimeters within 5 min. With linear trend removal, the drifts are reduced to only a few centimeters, and the standard deviations are reduced from 13.5, 2.5 and 24.3 cm to 0.9, 1.9 and 4.1 cm in the east, north and up components, respectively.

It is noticeable that non-linear trends remain in the displacements after linear trend removal. They can be mitigated using spatial filtering (Hung et al. 2017) or high-pass

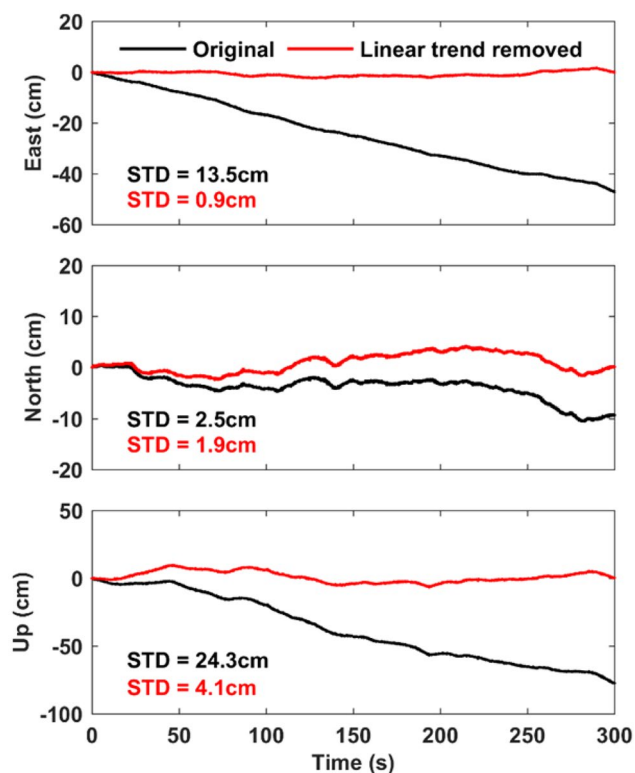


Fig. 2 Displacements at the station SCTQ during a static period previous to the Lushan earthquake derived using the variometric approach. The black lines represent the original displacements without linear trend removal, and the red lines represent the displacements with linear trend removal. The standard deviations are also shown in corresponding colors

filtering. However, these filtering techniques have the disadvantages of the need for close reference stations or the loss of low-frequency signals. Therefore, they are not adopted in this study.

When applying the linear-trend removal strategy to long-duration displacements exceeding a few minutes, e.g., coseismic displacements during the Tohoku-Oki earthquake under our study, non-linear drifts can be very large. In this case, we remove the linear trends in a piecewise way.

Comparison of 50 Hz and 1 Hz GPS results

All 15 GPS monitoring stations analyzed in our study successfully recorded 50 Hz data during the earthquakes. The data are processed to obtain 50 Hz displacements using the variometric approach. We also obtain 1 Hz displacements by processing 1 Hz GPS data decimated from 50 Hz ones. The linear trends are removed from the integrated displacements as mentioned above.

The comparison between 50 and 1 Hz incremental displacements, velocities and displacements at the station SCTQ during the Lushan earthquake is shown in Fig. 3. The seismic signals are clearly observable in both 50 Hz and 1 Hz results, starting at about 21 s after the origin and lasting about 27 s. The time series during the static period, namely the first 20 s and last 13 s in Fig. 3, represent the noises. The standard deviations of these noises are calculated and listed in Table 1. From Fig. 3 and Table 1 we find that the variometric approach can determine the incremental displacements with millimeter- or even submillimeter-level precision, and the precision in the up component is lower than the horizontal components by a factor of about 3. We also find that the precision of 50 Hz incremental displacements is higher than that of 1 Hz ones by a factor of about 2. This is probably because consecutive epochs during shorter intervals share more common-mode errors, and due to time differencing incremental displacements with higher sampling rates cancel the errors more thoroughly than those with lower sampling rates. The standard deviation of 50 Hz velocities is 3–9 cm/s, which is much larger than that of 1 Hz ones. This is reasonable because the velocities are obtained by dividing the incremental displacements by the sampling intervals. The noise level of 50 Hz velocities is amplified by 50 compared to the incremental displacements, whereas the noise level of 1 Hz velocities is the same as that of the incremental displacements.

Linear trends in the displacements in Fig. 3 are removed, but non-linear trends still remain and slightly affect the displacements. The effect of these non-linear trends is at sub-centimeter level, as can be seen from the standard deviations of the displacements during the static period in Table 1. The standard deviations of 50 Hz displacements are nearly the same as those of 1 Hz displacements. In the seismic period

Fig. 3 Comparison of 50 Hz and 1 Hz incremental displacements, velocities and displacements at station SCTQ during the 2013 M_w 6.6 Lushan earthquake. The upper, middle and lower panels represent the incremental displacements, velocities and displacements, respectively

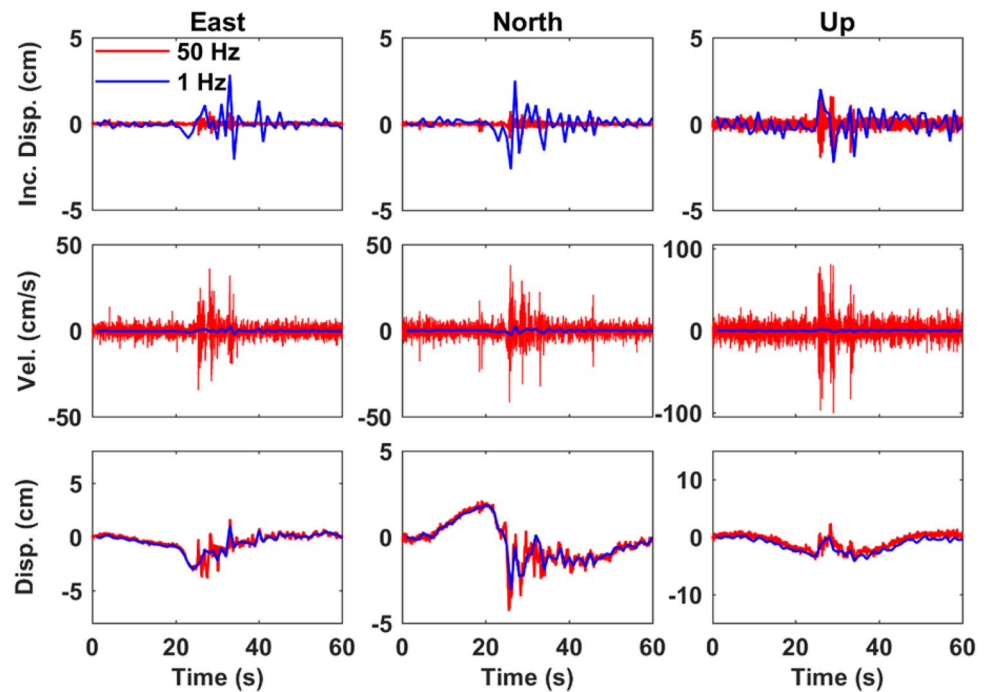


Table 1 Standard deviations of incremental displacements, velocities and displacements of SCTQ during the static period

Sampling rate	Incremental displacements (mm)			Velocities (mm/s)			Displacements (mm)		
	<i>E</i>	<i>N</i>	<i>U</i>	<i>E</i>	<i>N</i>	<i>U</i>	<i>E</i>	<i>N</i>	<i>U</i>
50 Hz	0.6	0.7	1.8	29.6	32.5	89.3	3.9	9.1	7.9
1 Hz	1.6	1.8	4.8	1.6	1.8	4.8	4.2	8.8	7.8

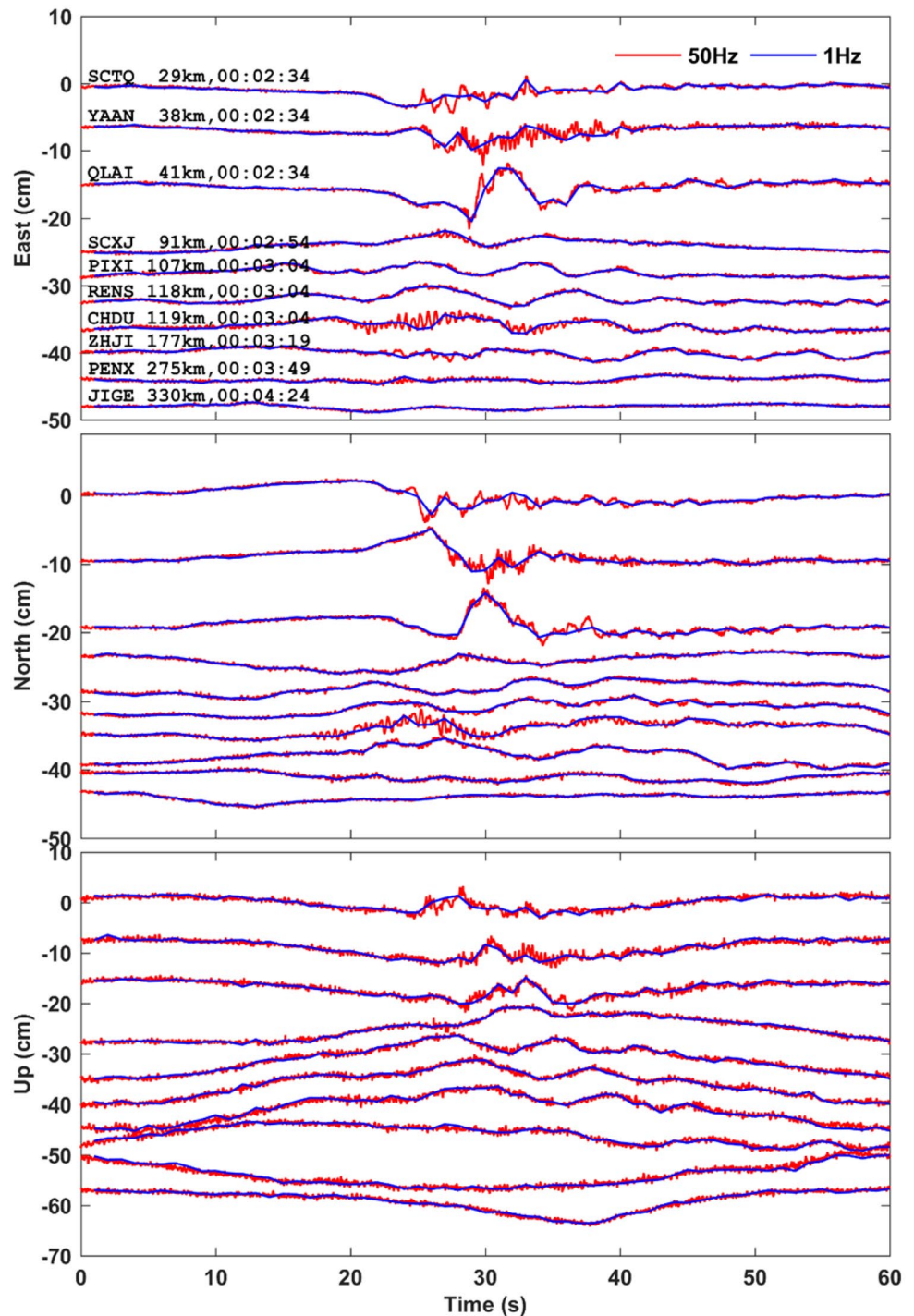
during 21–47 s, the waveform phase and amplitudes of seismic signals for 50 Hz and 1 Hz incremental displacements are totally different. For example, the maximum amplitude of the incremental horizontal displacements reaches 2.8 cm for 1 Hz results, whereas only 0.8 cm for 50 Hz results. This is because 50 Hz results represent incremental displacements of a much shorter time interval of 0.02 s than 1 Hz results, with the latter accumulating to larger incremental displacements within a longer time interval of 1 s. The amplitude of 50 Hz velocities is much larger than that of 1 Hz ones in the seismic period. In addition to the amplified noises in 50 Hz velocities, another reason is that 50 Hz velocities can be regarded as instantaneous velocities, whereas 1 Hz velocities are averaged over 1 s. Although the 1 Hz displacements have the same instantaneous amplitude at each sample as the 50 Hz displacements, as shown in Fig. 3, they fail to reflect the high-frequency components which can be clearly seen in the 50 Hz displacements. The aliasing problem occurs in the 1 Hz displacements.

The 50 Hz and 1 Hz coseismic displacements derived using the variometric approach during the Lushan earthquake and Tohoku-Oki earthquake are shown in Figs. 4 and

5, respectively. The 1 Hz coseismic velocities are also shown in Figures S1 and S2 in Online Resource. As shown in Fig. 4 and S1, during the Lushan earthquake, seismic waves first arrived at SCTQ, the closest station to the epicenter, then sequentially propagated to farther stations. Displacements of STCQ, YAAN and QLAI, the three closest stations to the epicenter, have the amplitudes of 4–7 cm and 2–6 cm in the horizontal and up components, respectively. The other 5 stations with epicentral distances less than 200 km have obvious seismic signals but with smaller amplitudes than the three closest stations. At the two farthest stations, very weak seismic signals can be observed from PENX, whereas no seismic signals are captured by JIGE.

During the static period in Fig. 4, 50 Hz and 1 Hz displacements at these stations overlap perfectly. During the seismic period, however, 1 Hz displacements are different from 50 Hz ones, especially in all three components of SCTQ, YAAN and QLAI and in horizontal components of CHDU and ZHJI. The comparisons between 50 and 1 Hz coseismic displacements show that most stations are affected by aliasing in the 1 Hz coseismic displacements. SCTQ, YAAN and QLAI are the three closest stations with nearly

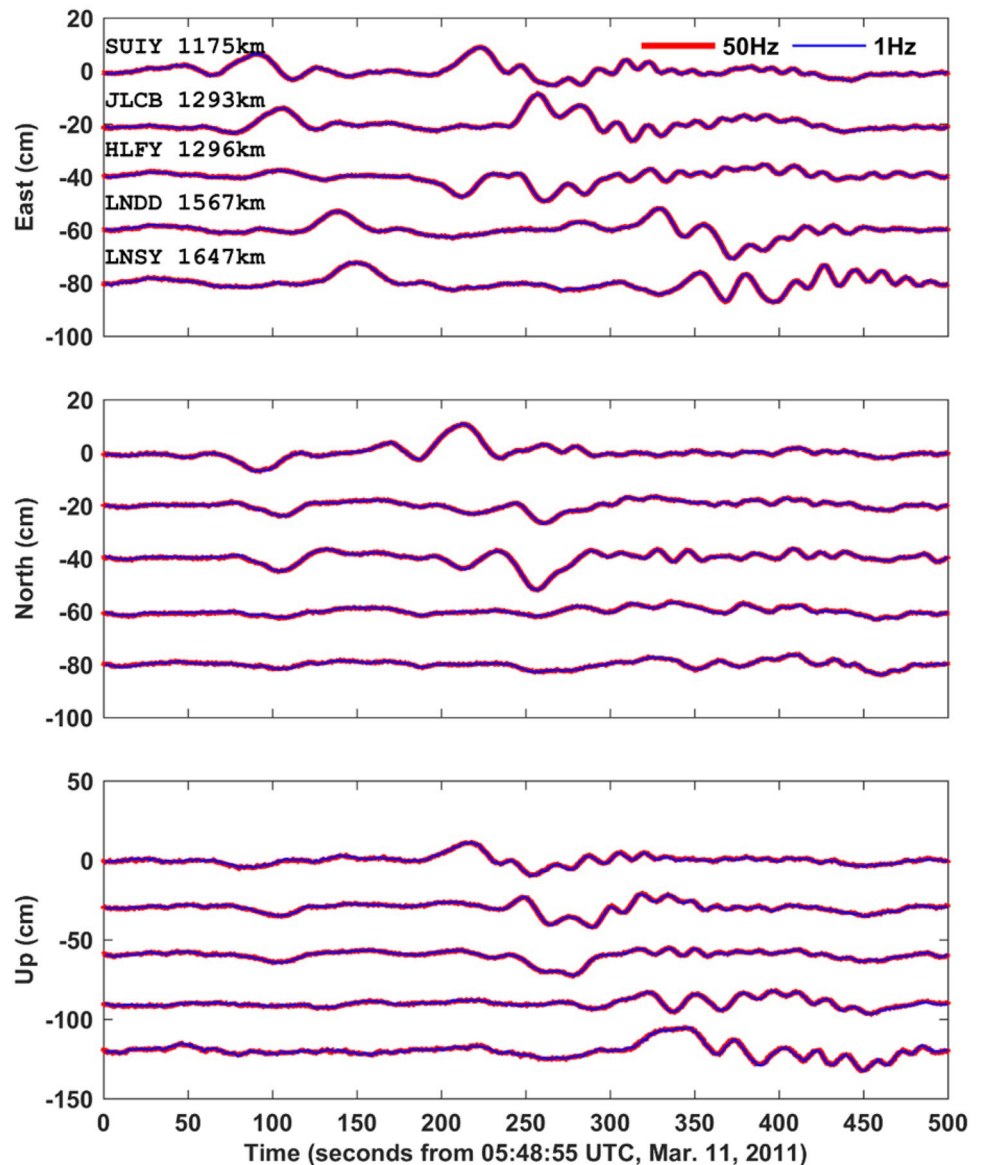
Fig. 4 Comparison of 50 Hz and 1 Hz coseismic displacements at 10 stations during the 2013 M_W 6.6 Lushan earthquake. Displacements in this figure are vertically shifted for clarity. Following the station name is the epicentral distance and starting time (UTC) on Apr. 20, 2013



equal epicentral distances. Their 1 Hz solutions are significantly affected by aliasing with amplitudes slightly smaller than those of 50 Hz ones. The remaining 7 stations are farther from the epicenter, and we can see that the vibration amplitudes at these stations are smaller due to attenuation of the high-frequency components on the longer travel path. However, they still experience more or less aliasing in the 1 Hz displacements except JIGE, the farthest site from the

epicenter. It is interesting to note that for the four stations SCXJ, PIXI, RENS and CHDU with nearly equal epicentral distances about 100 km, the vibration amplitude at CHDU is significantly larger than those at the other three stations. The possible reason for the amplification effects is that CHDU has a different soil condition and/or height of GPS antenna from the other three stations (Fang et al. 2014; Galetzka et al. 2015). These results demonstrate that 1 Hz

Fig. 5 Comparison of 50 Hz and 1 Hz coseismic displacements at 5 stations during the 2011 M_w 9.0 Tohoku-Oki earthquake. Displacements in this figure are vertically shifted for clarity. Following the station names are the epicentral distances



displacements in the near-field with epicentral distances shorter than 300 km of moderate earthquakes with the magnitude of 5–7 are easily affected by aliasing, in agreement with previous studies (Smalley 2009; Avallone et al. 2011). Those aliased solutions are inappropriate to be used for seismic spectrum analyses or inversions for source parameters (Smalley 2009). To reconstruct alias-free near-field seismic waves caused by moderate or large earthquakes, we suggest that it is necessary to equip monitoring GPS stations with very high-rate receivers.

As a comparison to the Lushan earthquake, Fig. 5 demonstrates the 50 Hz and 1 Hz coseismic displacements at 5 stations during the M_w 9.0 Tohoku-Oki earthquake. The 1 Hz coseismic velocities are also shown in Figure S2. These stations are located in northeast China with epicentral distances longer than 1000 km, which are much farther

compared to those stations recording the Lushan earthquake. The seismic waves at these stations are governed by low-frequency components below 0.2 Hz, as discussed in the following spectral analysis. Most high-frequency seismic signals have attenuated before arriving at these stations due to the very long propagation paths. By comparing 50 Hz and 1 Hz displacements in Fig. 5, we find that they overlap perfectly throughout the entire time series, whether in the static or seismic period. This phenomenon indicates that 1 Hz displacements in the far-field of earthquakes are not affected by aliasing, even for earthquakes with the magnitude as large as M_w 9.0.

To investigate the frequency contributions of the 50 Hz and 1 Hz displacements, we estimated their power spectral densities (PSDs). We calculated PSDs of displacements before the earthquake occurrence, denoted as the

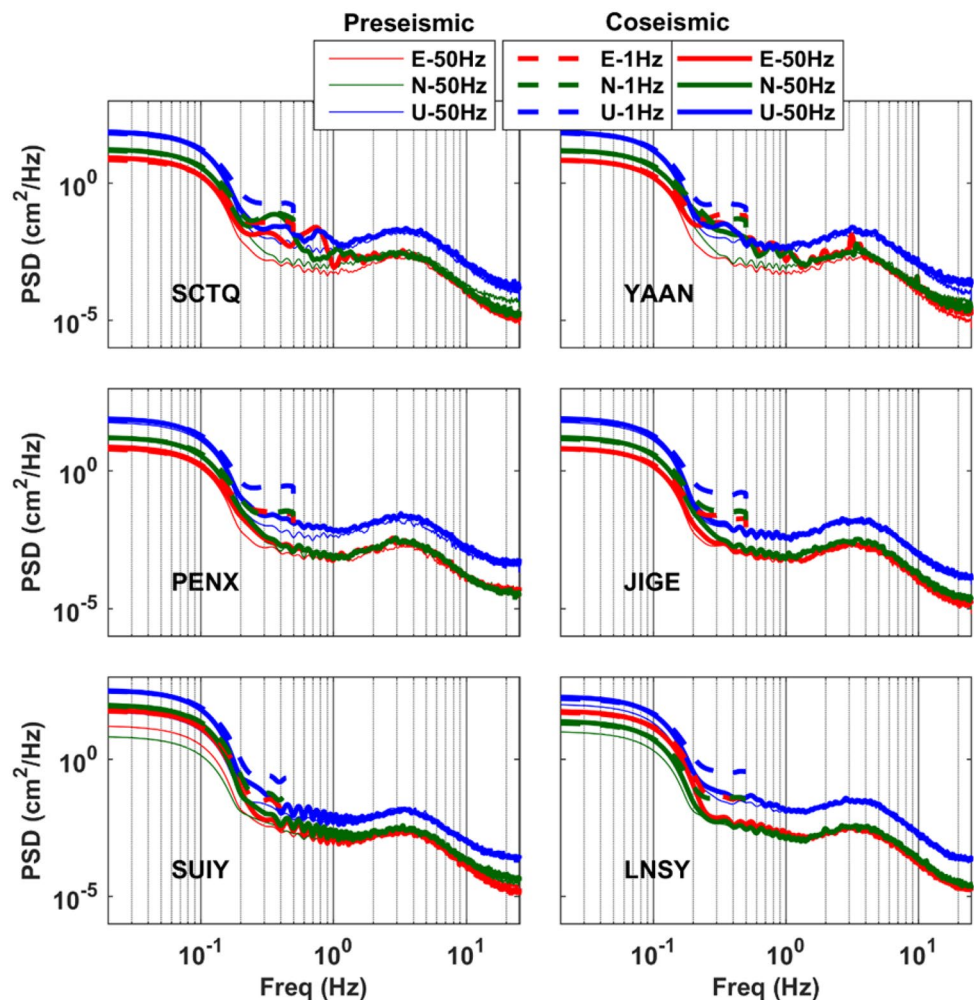
“preseismic” stage in this study, for 50 Hz solutions, as well as PSDs of displacements during the earthquake, denoted as the “coseismic” stage in this study, for both 50 Hz and 1 Hz solutions. When calculating preseismic or coseismic PSDs, 15-min length of data were used. We chose 6 representative stations, SCTQ, YAAN, PENX, JIGE, SUIY and LNSY in our PSD analysis, as shown in Fig. 6. SCTQ, YAAN, PENX and JIGE recorded the Lushan earthquake, whereas SUIY and LNSY recorded the Tohoku-Oki earthquake.

The preseismic PSDs of these 6 stations exhibit the same general shape, representing the noise levels of GPS. Below 0.1 Hz, preseismic PSDs decrease very slowly as the frequency increases. At the frequency range of 0.1–0.2 Hz, preseismic PSDs of all 6 stations decrease with increasing slope. At the frequency range of 0.2–1 Hz, preseismic PSDs undergo an approximately linear decline. Above 1 Hz, however, PSDs begin to increase until the transition at a frequency of about 3.5 Hz. Above this transition frequency, another decline with decreased slope takes place. The east and north components have comparable noise levels. The up

component has much higher noise levels than the horizontal components, as expected, considering the generally higher precision of the horizontal components in GPS positioning. The noises at frequencies above 1 Hz are primarily caused by receiver electronic noises. These high-frequency noises have a non-white behavior, similar to the 50 Hz DGPS (differential GPS) solutions presented by Niu et al. (2013). Their correlation in time is probably caused by the low-pass effect of the carrier phase tracking loop inside the receiver (Niu et al. 2013).

The differences between the 50 Hz coseismic PSDs and preseismic PSDs reflect the seismic signals. SCTQ and YAAN are the two closest stations to the epicenter among the 10 stations in our study recording the Lushan earthquake, and their seismic signals cover a wide range of frequencies, generally between 0.1 and 3 Hz in all three components. Many spectral peaks can be found in the seismic signals, especially for SCTQ at 0.7, 0.4 and 0.8 Hz in the east, north and up components, respectively. PENX and JIGE are the two farthest stations to the epicenter among the 10 stations recording the Lushan earthquake. Compared

Fig. 6 PSDs of 6 representative stations, with SCTQ, YAAN, PENX and JIGE recording the Lushan earthquake, and SUIY and LNSY recording the Tohoku-Oki earthquake. The thin solid lines represent the preseismic PSDs for 50 Hz solutions before the earthquake, the thick solid lines and dashed lines represent the coseismic PSDs for 50 and 1 Hz solutions, respectively, containing the seismic waves



with SCTQ and YAAN, PENX has less seismic energy and no spectral peaks can be found, whereas no seismic energy exists at the station JIGE. SUIY and LNSY are the closest and farthest stations to the epicenter among the 5 stations in our study recording the Tohoku-Oki earthquake. Their seismic signals mainly cover the frequency range below 0.5 Hz, and no spectral peaks exist in the seismic signals, indicating that those stations recording the Tohoku-Oki earthquake only contain low-frequency seismic signals, which can also be indicated by the displacement time series in Fig. 5.

1 Hz coseismic PSDs are also shown in Fig. 6 for the comparison with 50 Hz ones. All the 1 Hz coseismic PSDs well overlap with 50 Hz ones at frequencies below 0.1 Hz. However, at frequencies between 0.1 and 0.5 Hz, 1 Hz coseismic PSDs are larger than 50 Hz ones, this is because high-frequency seismic signals or/and non-seismic noises are aliased into the 1 Hz coseismic PSDs. This phenomenon reflects the aliasing problem in the 1 Hz coseismic displacements from the perspective of the frequency domain.

Comparison with post-processed PPP displacements

To assess the quality of the displacements derived using the variometric approach, we compare them with the 50 Hz post-processed PPP displacements derived using the PANDA software developed by Wuhan University (Shi et al. 2008). In the PPP processing, dual-frequency code and phase observations are used to eliminate the first-order ionospheric errors. Precise satellite orbit with the 15-min interval and clock products with the 5-s interval from CODE (Center for Orbit Determination in Europe) are used.

The comparison of displacements derived using the variometric approach and PPP, for 3 stations during the Lushan earthquake is shown in Fig. 7. The displacements derived using the variometric approach are affected by non-linear trends due to the integration process and deviate from PPP displacements to some extent. However, the short-term waveforms derived using the two techniques are well consistent with each other.

Taking the PPP displacements as references, we calculated the root mean square errors (RMSEs) of the displacements derived using the variometric approach for all stations separately for the preseismic and coseismic displacements. Considering the time duration of coseismic displacements for the two earthquakes, we calculated the RMSEs using 60-s and 500-s time windows for the Lushan earthquake and the Tohoku-Oki earthquake, respectively. The RMSEs for each station and the mean RMSEs for the Lushan earthquake and the Tohoku-Oki earthquake are listed in Table 2. Compared with post-processed PPP, the variometric approach can retrieve seismic displacements with accuracies of 0.3–4.1, 0.5–2.3 and 0.8–6.8 cm in the

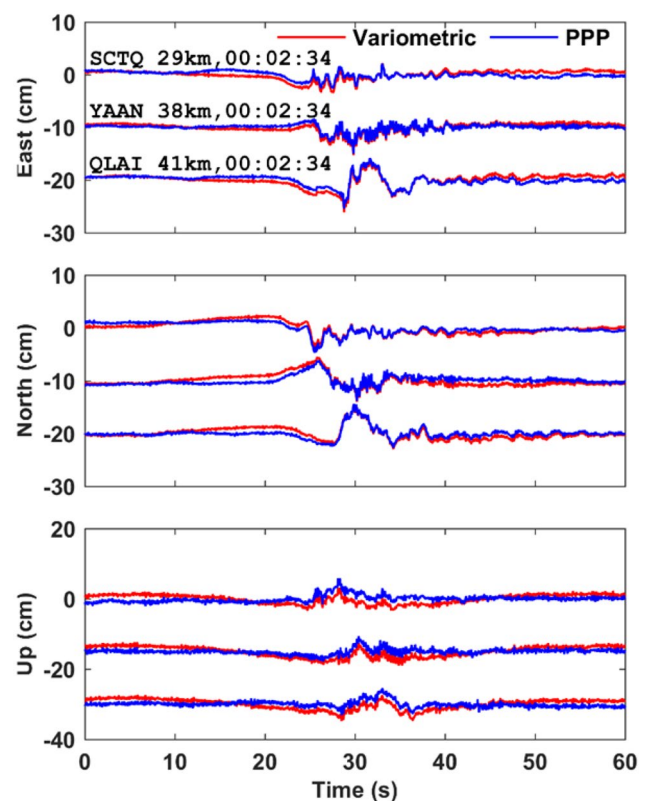


Fig. 7 Comparison of 50 Hz displacements between the variometric approach and PPP for stations SCTQ, YAAN and QLAI during the 2013 M_w 6.6 Lushan earthquake. Displacements in this figure are vertically shifted for clarity. Following the station name are the epicentral distance and starting time (UTC) on Apr. 20, 2013

east, north and up components, respectively. The RMSEs of the east component is comparable with that of the north component, whereas the up component is larger than the horizontal components by a factor of about 3. The RMSEs for the Tohoku-Oki earthquake are larger than those for the Lushan earthquake, indicating that the stations recording the Tohoku-Oki earthquake are more largely affected by non-linear trends. The RMSEs of the coseismic displacements are slightly larger than those of the preseismic displacements, indicating that the consistence level of the two techniques in the seismic period is lower than that in the static period. Generally speaking, the displacements derived using the variometric approach agree with PPP within centimeter to sub-centimeter level in both static and seismic periods.

To further compare the results from the variometric approach and PPP, we calculated the PSDs of coseismic displacements. 15-min length of coseismic displacements were used to calculate the PSDs. Figure 8 shows the coseismic PSDs of 6 representative stations. The coseismic PSDs of these two datasets have a similar shape in all three components. At frequencies below 0.2 Hz, the PSDs from these

Table 2 Root mean square errors (cm) of the displacements derived using the variometric approach referred to PPP displacements

	Preseismic			Coseismic		
	<i>E</i>	<i>N</i>	<i>U</i>	<i>E</i>	<i>N</i>	<i>U</i>
Lushan earthquake (60-s time window)						
SCTQ	0.4	0.7	1.6	0.7	0.5	1.6
YAAN	0.3	0.6	1.7	0.5	0.8	1.3
QLAI	0.3	0.6	1.6	0.7	0.6	1.5
SCXJ	0.3	0.7	1.4	0.6	0.7	2.2
PIXI	0.3	0.6	0.7	0.6	0.8	2.6
RENS	0.2	0.7	1.2	0.4	0.7	2.4
CHDU	0.3	0.6	1.4	0.5	0.8	2.2
ZHJI	0.5	0.6	1.2	0.2	0.9	1.9
PENX	0.5	0.6	1.9	0.2	0.4	1.9
JIGE	0.2	1.0	1.1	0.3	0.4	1.7
Mean value	0.3	0.7	1.4	0.5	0.7	1.9
Tohoku-Oki earthquake (500-s time window)						
SUIY	0.9	0.7	2.7	2.5	1.7	3.0
JLCB	0.9	0.8	2.2	2.4	1.7	3.3
HLFY	0.8	0.7	2.0	4.0	1.9	2.1
LNDD	1.3	0.9	2.7	1.6	2.3	4.4
LNSY	1.3	1.3	4.1	3.0	2.1	6.7
Mean value	1.0	0.9	2.7	2.7	1.9	3.9

two datasets do not overlap because of the low-frequency non-linear trends in the displacements from the variometric approach. At frequencies above 10 Hz, PSDs of PPP results are larger than those derived from the variometric approach, indicating that PPP results have larger high-frequency noises than the results derived using the variometric approach. This is reasonable, considering that the ionosphere-free combination is used in PPP, which amplifies the noise of raw carrier phase by a factor of about 3. In the variometric approach, this amplification is only about 1.414, because it uses single-differencing over time of single-frequency carrier phase observations in our study.

Conclusions

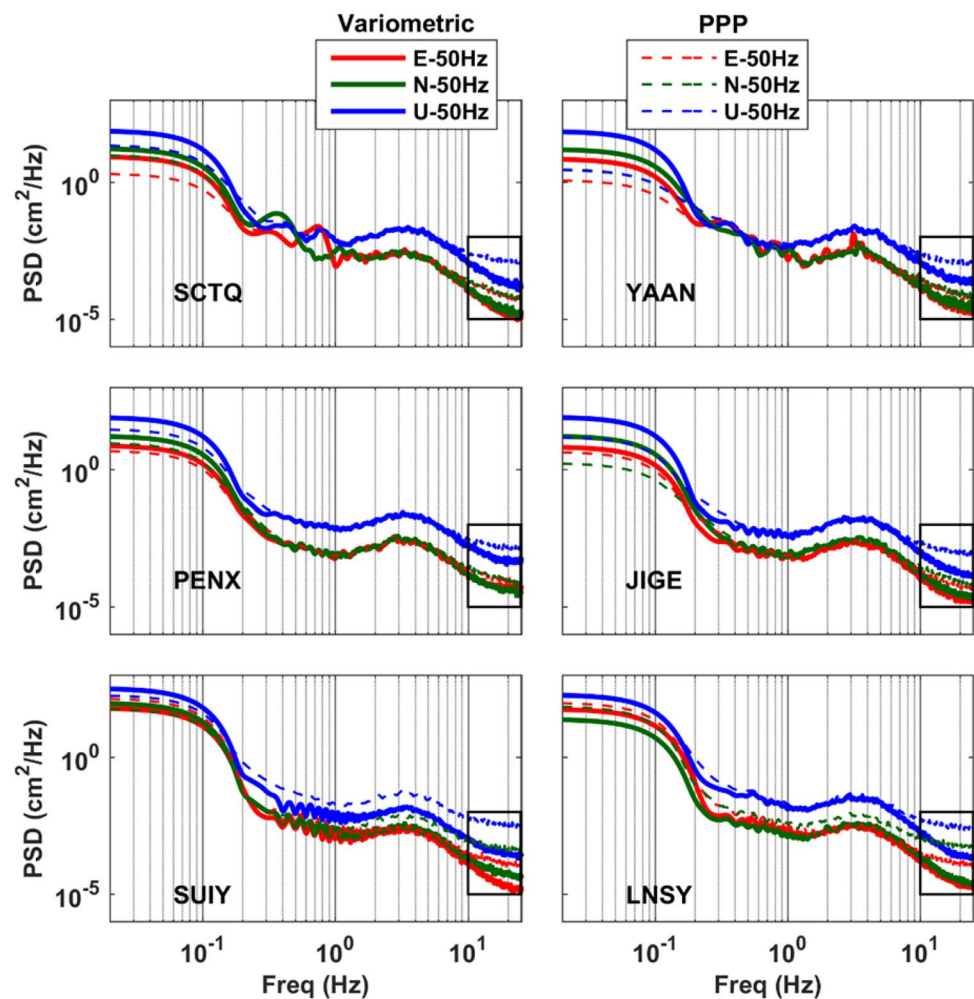
We evaluate the performance of the variometric approach to measure dynamic seismic displacements using very high-rate GPS data with the sampling rate of 50 Hz, which were recorded during the 2013 M_W 6.6 Lushan earthquake and the 2011 M_W 9.0 Tohoku-Oki earthquake.

The comparison between 50 and 1 Hz coseismic displacements derived using the variometric approach indicates that 1 Hz displacements in the near-field of moderate-magnitude

earthquakes are easily affected by aliasing. Stations closer to the epicenter are more affected by aliasing, because they contain more high-frequency components. As the epicentral distance increases, 1 Hz displacements are less affected by aliasing due to attenuation of the high-frequency components on the longer travel path. Therefore, to reconstruct near-field seismic waves caused by moderate or large earthquakes, it is helpful to equip monitoring stations with very high-rate GPS receivers.

The displacements derived using the variometric approach are compared with post-processed PPP displacements. An agreement within centimeter to sub-centimeter level in three components was demonstrated, no matter in the static or seismic period. Noises of displacements at frequencies above 10 Hz from the variometric approach are found to be smaller than those of PPP displacements. The variometric approach can achieve comparable precision with PPP while eliminating the requirements indispensable to PPP, i.e., precise orbit/clock products, elaborate error corrections, ambiguity estimation and a long convergence time. In addition, the variometric approach supports real-time or near real-time applications. Therefore, the variometric approach is a viable alternative to measure high-rate, i.e., 1–5 Hz, or even very high-rate, i.e., 10–50 Hz ground displacements.

Fig. 8 Power spectral densities (PSDs) of the 50 Hz coseismic displacements derived using the variometric approach and PPP for 6 stations, with SCTQ, YAAN, PENX and JIGE recording the Lushan earthquake, and SUIY and LNSY recording the Tohoku-Oki earthquake. The black boxes contain the PSDs above 10 Hz

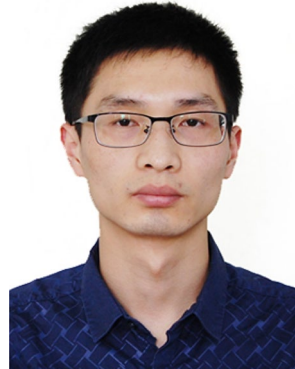


Acknowledgements This work is supported by the National Natural Science Foundation of China (Nos. 41631073, 41874038, 41231174 and 41325015). We thank two anonymous reviewers and the Editor Alfred Leick, for their detailed and constructive comments which significantly improved the manuscript.

References

- Allen RM, Ziv A (2011) Application of real-time GPS to earthquake early warning. *Geophys Res Lett* 38:L16310
- Avallone A et al (2011) Very high rate (10 Hz) GPS seismology for moderate-magnitude earthquakes: The case of the M_w 6.3 L'Aquila (central Italy) event. *J Geophys Res* 116:B02305
- Benedetti E, Branzanti M, Biagi L, Colosimo G, Mazzoni A, Crespi M (2014) Global navigation satellite systems seismology for the 2012 M_w 6.1 Emilia earthquake: exploiting the VADASE algorithm. *Seismol Res Lett* 85(3):649–656
- Bilich A, Cassidy JF, Larson KM (2008) GPS seismology: application to the 2002 M_w 7.9 Denali fault earthquake. *B Seismol Soc Am* 98(2):593–606
- Bock Y, Prawirodirdjo L, Melbourne TI (2004) Detection of arbitrarily large dynamic ground motions with a dense high-rate GPS network. *Geophys Res Lett* 31(6):L06604
- Bock Y, Melgar D, Crowell BW (2011) Real-time strong-motion broadband displacements from collocated GPS and accelerometers. *Bull Seismol Soc Am* 101(6):2904–2925
- Branzanti M, Colosimo G, Crespi M, Mazzoni A (2013) GPS near-real-time coseismic displacements for the great Tohoku-oki earthquake. *IEEE Geosci Remote Sens Lett* 10(2):372–376
- Celebi M, Sanli A (2002) GPS in pioneering dynamic monitoring of long-period structures. *Earthquake Spectra* 18(1):47–61
- Colombelli S, Allen RM, Zollo A (2013) Application of real-time GPS to earthquake early warning in subduction and strike-slip environments. *J Geophys Res* 118(7):3448–3461
- Colosimo G, Crespi M, Mazzoni A (2011) Real-time GPS seismology with a stand-alone receiver: a preliminary feasibility demonstration. *J Geophys Res* 116:B11302
- Crowell BW, Bock Y, Squibb MB (2009) Demonstration of earthquake early warning using total displacement waveforms from real-time GPS networks. *Seismol Res Lett* 80(5):772–782
- Fang R, Shi C, Song W, Wang G, Liu J (2014) Determination of earthquake magnitude using GPS displacement waveforms from real-time precise point positioning. *Geophys J Int* 196(1):461–472
- Fratarcangeli F, Savastano G, D'Achille M, Mazzoni A, Crespi M, Riguzzi F, Devoti R, Pietrantonio G (2018) VADASE reliability and accuracy of real-time displacement estimation: application to the Central Italy 2016 earthquakes. *Remote Sens* 10(8):1201

- Galetzka J et al (2015) Slip pulse and resonance of the Kathmandu basin during the 2015 Gorkha earthquake, Nepal. *Science* 349(6252):1091–1095
- Geng T, Xie X, Fang R, Su X, Zhao Q, Liu G, Li H, Shi C, Liu J (2016) Real-time capture of seismic waves using high-rate multi-GNSS observations: Application to the 2015 M_w 7.8 Nepal earthquake. *Geophys Res Lett* 43(1):161–167
- Genrich JF, Bock Y (2006) Instantaneous geodetic positioning with 10–50 Hz GPS measurements: noise characteristics and implications for monitoring networks. *J Geophys Res* 111(B3):B03403
- Grapenthin R, Freymueller JT (2011) The dynamics of a seismic wave field: animation and analysis of kinematic GPS data recorded during the 2011 Tohoku-oki earthquake, Japan. *Geophys Res Lett* 38:L18308
- Heroux P, Kouba J (2001) GPS precise point positioning using IGS orbit products. *Phys Chem Earth* 26(6–8):573–578
- Hung H-K, Rau R-J, Benedetti E, Branzanti M, Mazzoni A, Colosimo G, Crespi M (2017) GPS Seismology for a moderate magnitude earthquake: Lessons learned from the analysis of the 31 October 2013 ML 6.4 Ruisui (Taiwan) earthquake. *Ann Geophys* 60(5):S0553
- Kouba J (2003) Measuring seismic waves induced by large earthquakes with GPS. *Stud Geophys Geod* 47(4):741–755
- Larson KM (2009) GPS seismology. *J Geod* 83(3–4):227–233
- Larson KM, Bodin P, Gomberg J (2003) Using 1 Hz GPS data to measure deformations caused by the Denali fault earthquake. *Science* 300(5624):1421–1424
- Li X, Guo B, Lu C, Ge M, Wickert J, Schuh H (2014) Real-time GNSS seismology using a single receiver. *Geophys J Int* 198(1):72–89
- Melgar D, Crowell BW, Geng J, Allen RM, Bock Y, Riquelme S, Hill EM, Protti M, Ganas A (2015) Earthquake magnitude calculation without saturation from the scaling of peak ground displacement. *Geophys Res Lett* 42(13):5197–5205
- Miyazaki S, Larson KM, Choi K, Hikima K, Koketsu K, Bodin P, Haase J, Emore G, Yamagiwa A (2004) Modeling the rupture process of the 2003 September 25 Tokachi-Oki (Hokkaido) earthquake using 1 Hz GPS data. *Geophys Res Lett* 31:L21603
- Moschas F, Stiros S (2015) Dynamic deflections of a stiff footbridge using 100 Hz GNSS and accelerometer data. *J Surv Eng* 141(4):04015003
- Niu X, Chen Q, Zhang Q, Zhang H, Niu J, Chen K, Shi C, Liu J (2013) Using Allan variance to analyze the error characteristics of GNSS positioning. *GPS Solut* 18(2):231–242
- Nyquist H (1928) Certain topics in telegraph transmission theory. *Trans Am Inst Electr Eng* 47(2):617–644
- Ogaja C, Li X, Rizos C (2007) Advances in structural monitoring with global positioning system technology: 1997–2006. *J Appl Geodesy* 1(3):171–179
- Ohta Y et al (2012) Quasi real-time fault model estimation for near-field tsunami forecasting based on RTK-GPS analysis: application to the 2011 Tohoku-Oki earthquake (M_w 9.0). *J Geophys Res* 117:B02311
- Shi C, Zhao Q, Geng J, Lou Y, Ge M, Liu J (2008) Recent development of PANDA software in GNSS data processing. In: Proceedings of international conference on Earth observation data processing and analysis (ICEODPA). Wuhan, China, 28–30 December, p 72851S
- Smalley R (2009) High-rate GPS: how high do we need to go? *Seismol Res Lett* 80(6):1054–1061
- Wright TJ, Houlie N, Hildyard M, Iwabuchi T (2012) Real-time, reliable magnitudes for large earthquakes from 1 Hz GPS precise point positioning: the 2011 Tohoku-Oki (Japan) earthquake. *Geophys Res Lett* 39:L12302
- Xu P, Shi C, Fang R, Liu J, Niu X, Zhang Q, Yanagidani T (2013) High-rate precise point positioning (PPP) to measure seismic wave motions: An experimental comparison of GPS PPP with inertial measurement units. *J Geod* 87(4):361–372
- Yin H, Wdowinski S (2013) Improved detection of earthquake-induced ground motion with spatial filter: case study of the 2012 $M = 7.6$ Costa Rica earthquake. *GPS Solut* 18(4):563–570
- Zumberge J, Heflin M, Jefferson D, Watkins M, Webb F (1997) Precise point positioning for the efficient and robust analysis of GPS data from large networks. *J Geophys Res* 102(B3):5005–5017



Yuanming Shu is currently a Ph.D. candidate at GNSS Research Center of Wuhan University, China. He received his B.E. degree in geodesy and geomatics engineering from School of Geodesy and Geomatics of Wuhan University in 2013. His current research mainly focuses on GNSS high-precision positioning, GNSS attitude determination and GNSS/INS integration.



Rongxin Fang is currently an associate professor at GNSS Research Center in Wuhan University, China. He obtained his Ph.D. in geodesy and surveying engineering at Wuhan University in 2010. Then he finished 2 years postdoctoral research at GNSS Research Center in Wuhan University from 2011 to 2013. His main research interests include precise point positioning and GNSS seismology.



Min Li is currently a professor at GNSS Research Center of Wuhan University, China. He obtained his Ph.D. in geodesy and surveying engineering in Wuhan University in 2011. His main work focuses on GNSS satellite orbit determination and precise point positioning as well as multi-GNSS processing using GPS, GLONASS, COMPASS and Galileo.



Chuang Shi is the professor at GNSS Research Center, Wuhan University and School of Electronic and Information Engineering, Beihang University. He graduated from Wuhan University and obtained his Ph.D. degree in 1998. His research interests include network adjustment, precise orbit determination of GNSS satellites and LEOs and real-time precise point positioning.



Jingnan Liu graduated from the former Wuhan College of Surveying and Mapping in 1967 and received his master's degree in 1982. He was elected Academician of the Chinese Academy of Engineering in 1999. Since 1998, he has been in charge of the National Engineering Research Center for Satellite Positioning System. His current research interests are satellite precise orbit determination and large-scale GNSS network adjustment theory and applications.



Meng Li is currently a lecturer at Faculty of Geomatics, East China University of Technology. He obtained his Ph.D. in Geodesy and Surveying Engineering at Southwest Jiaotong University in 2014. His main research interests include GNSS seismology and high-precision GNSS data processing.